# Chapter 3. Design and Implementation of Multimode Fiber-Based SCIIB Sensor System

This chapter will describe the design and implementation of the Multimode Fiber-Based SCIIB fiber optic sensor system. The multimode fiber-based SCIIB sensor system is developed for working for short distance applications at a low cost.

## 3.1 Multimode Optical Fiber Sensor

Of the properties of light which can be conveniently modulated, phase and polarization information are immediately lost upon entering a multimode optical fiber [22]. This leaves intensity as the only transmittable property available for use as a modulation sensitive parameter. However, even intensity is not well conserved in an optical fiber because of variable attenuation effects. As a result the development of multimode fiber sensing is concerned with producing various amplitude or intensity modulation methods and with overcoming the problems associated with the lack of intensity conservation.

Both analog and digital systems are available. Multimode sensors include varieties which are simple and inexpensive in their basic form, so they are potentially attractive for cost effective, bulk applications [23]. The modulators can be of relatively large dimensions, so large cored fibers can be employed, which improves tolerances with respect to end effects and so facilitates interconnections. As a result higher optical efficiencies are achievable and more flexible system architectures may be realized.

The performance criteria for a measurement system may be identified from a consideration of the characteristic which relates the output of the measurement system to the measurand value, such as the sensitivity, noise, signal-to-noise ratio, resolution, dynamic range and accuracy.

### 3.2 Multimode Fiber-Based SCIIB Fiber Optic Sensor System

The multimode fiber-based SCIIB sensor system is developed for relatively short distance applications at a low cost. As we know, multimode fibers have bigger loss than single-mode one when transmitting optical signals. Therefore, short distance applications are the major operating areas for multimode sensor system. Meanwhile in multimode fiber optic sensor systems infrared wavelength region (for example 850nm) is the most common used region that has much cheaper related optical components than those wavelength regions used for single-mode sensor systems (for example 1300nm or 1550nm). Thus the multimode fiber-based sensor system is more cost-efficient than the single-mode one. Along with the cost-efficiency multimode sensor systems are more convenient and easy for us to design and implement.

By utilizing different sorts of sensor heads, the multimode fiber-based SCIIB sensor system can be used for measurements of many physical or chemical measurands such as temperature, pressure, strain, displacement, etc. In the multimode system, light may be coupled more efficiently from the optical source into the multimode fiber whose core is much bigger than single-mode one. Hence a Light Emitting Diode(LED) can be employed in the system instead of a Super Luminescent Diode(SLD) and the cost can be reduced significantly; also the spectrum of a LED is generally wider and smoother than that of SLD, which is preferred in the system for more precision measurement with higher resolution.

### 3.3 Configuration and Operation of Multimode Fiber-Based SCIIB Sensor System

The schematic design of the multimode fiber-based SCIIB sensor system instrument box is shown in Figure 3-1, and the photo of the system is shown in Figure 3-2.

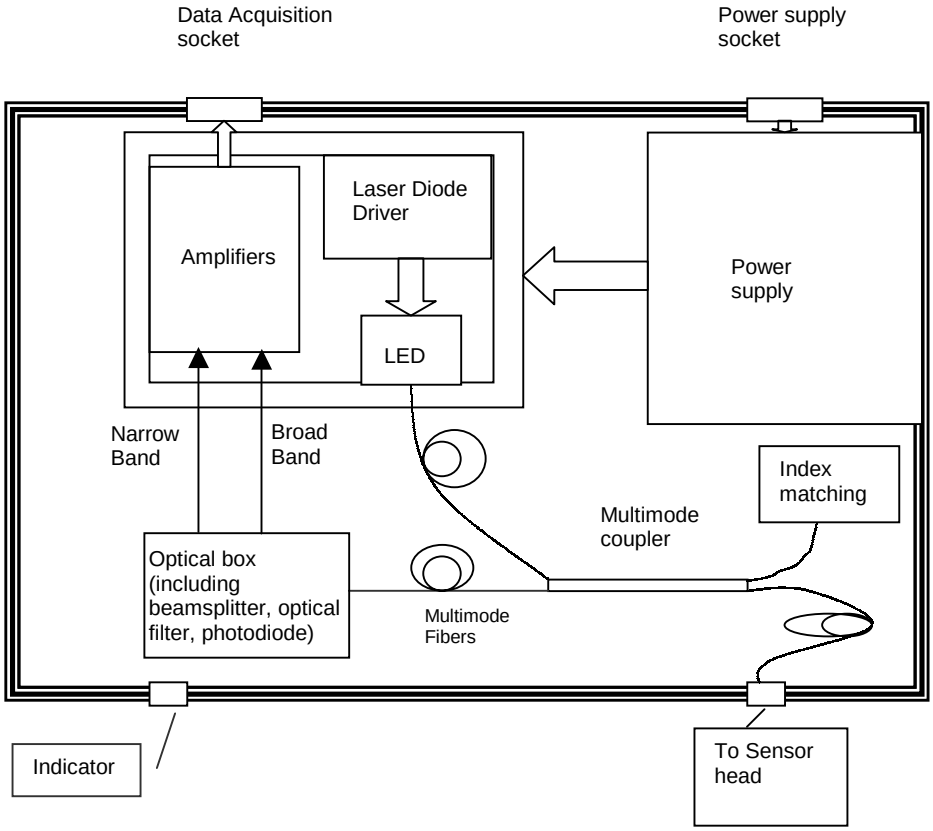


Figure 3-1. Schematic of the multimode SCIIB sensor system instrument box

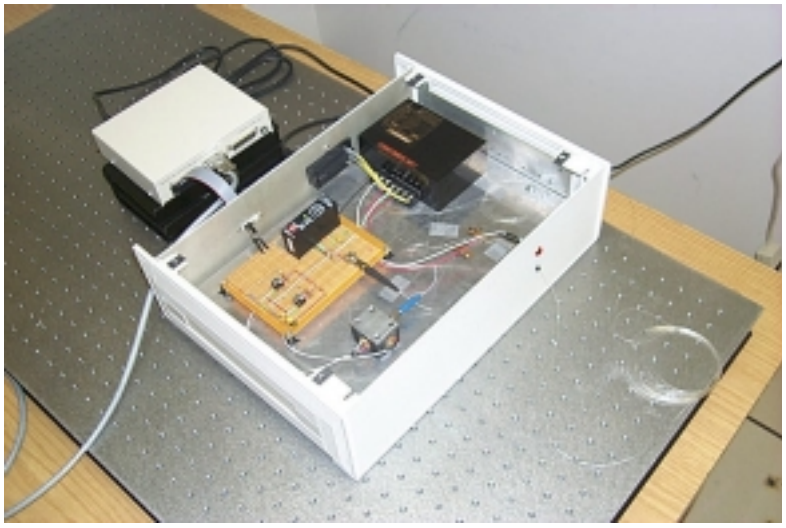

Figure 3-2. Photo of the multimode SCIIB fiber optic sensor system

The multimode fiber-based SCIIB fiber optic sensor system is developed to operate at the central wavelength of 850 nm. We use a LED as the broadband optical source, spectral width of around 90 nm, and the typical output power of 120 μW from the 62.5/125μm pigtailed multimode fiber. Because larger bandwidth of the optical source, smaller the F-P cavity length needed to implement the Split-Spectrum technique (the coherence length of the Broad Band will be smaller), as discussed in chapter 2. Meanwhile the spectrum of non-coherent LED is wider and smoother than that of partial-coherent SLD, and another benefit is that LED is significant cheaper than SLD.

We use 62.5μm/125μm standard telecommunication multimode optical fibers and a 3-dB coupler @ 850nm in the multimode SCIIB sensor system. Before the light beam reflected from the sensor head is split into two channels, a GRIN lens adhering to the end face of the output connector is used to collimate the output light beam. Then a polarization insensitive cubic beamsplitter with the splitting ratio of 50:50 is used to split the light output from the fiber into two channels. One channel passes through an optical bandpass filter with the central wavelength of 850 nm and the Full Width at the Half Maximum (FWHM) of 10 nm. This channel refers to the signal channel — Narrow Band. The other channel with the original spectrum of the LED refers to the reference channel — Broad Band. Two silicon photodiodes are used to receive the signals of the two channels. With the photodiodes of large effective areas (31 $mm^2$) it is convenient for us to align the optical circuit. After the opto-electronic conversion, the two channels' electronic signals are amplified by two trans-impedance amplifiers. Then the two amplified signals are sampled and converted to digital data by a data acquisition system including a high-precision A/D converter. Finally the digital signals are input to a computer where the ratio of these two channel signals is calculated for the final result.

### 3.4 Design and Implementation of Optical Circuit

The optical circuit part consists of the following components:

(1) LED @ 850nm(Honeywell Corp., HEF 4854-014)

(2) Multimode 62.5/125μm Fiber @ 850nm (SpecTran Specialty Optics Company, BF04431-02)

(3) 3-dB coupler @ 850nm (MP Fiberoptics, Inc.)

(4) Beamsplitter @ 850nm (Melles Griot, Inc., BF04431-02)

(5) GRIN Lens 0.25 pitch @ 850nm (Melles Griot, Inc., 06LGS216)

(6) Optical interference filter 10nm @ 850nm (CVI Laser Corp., BF04431-02)

(7) Silicon photodiode @ 850nm (Melles Griot, Inc., 13DSI009)

- **Power Budget**

The optical circuit part of the SCIIB fiber optic sensor system is shown in Figure 3-3 for reference. Now we will calculate the optical power at different places in the SCIIB sensor system.

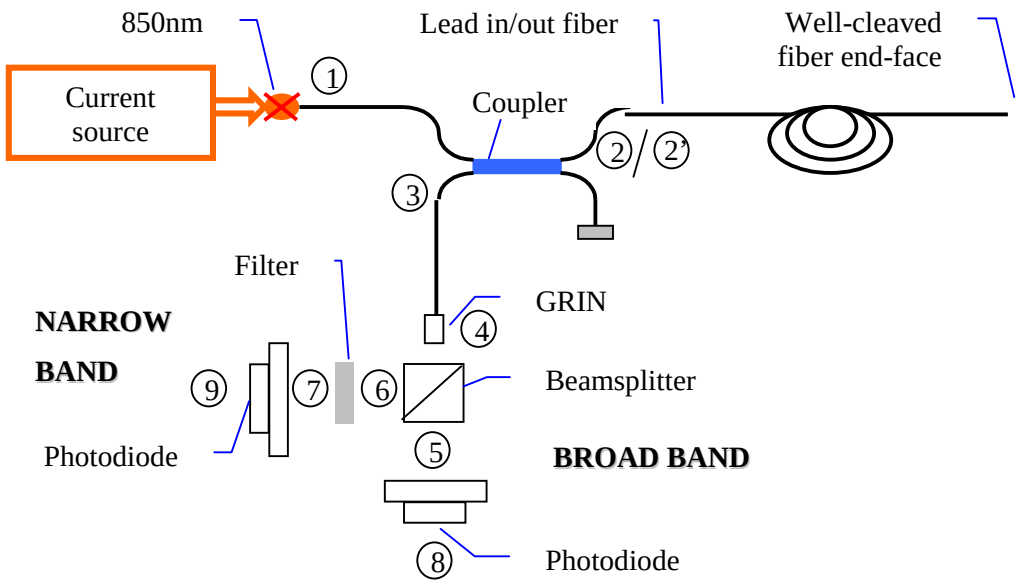


Figure 3-3 Multimode SCIIB System Analysis Model

1) Position 1: Under the worst condition, the optical power coupled into one branch of the 62.5/125um coupler is given by

$$P1=80\mu w$$

2) Position 2: Optical power that enters one branch of the coupler in the other side is given by

$$P2=P1*50\% =80*50\% =40\mu w$$

Attenuation Cause: 50% attenuation caused by the 3-dB coupler

3) Position 2': Optical power reflected from the end-face of the well-cleaved fiber without sensor head is given by

$$P2'=P2*4\% =40*4\% =1.6\mu w$$

Attenuation Cause: 4% reflectivity at the well-cleaved fiber end-face

4) Position 3: Reflected optical power output from one branch of the coupler is given by

$$P3=P2'*50\% =1.6*50\% =0.8\mu w$$

Attenuation Cause: 50% attenuation caused by 3-dB coupler

5) Position 4: Optical power output from GRIN is given by

$$P4\approx P3 =0.8\mu w$$

Attenuation Cause: there should be small attenuation caused by sticking GRIN to the end-face of FC connector, just ignore this small attenuation

6) Position 5 and 6: Output optical power split by beamsplitter is given by

$$P5=P6=P4*45\% =0.8*45\% =0.36\mu w$$

Attenuation Cause: split and absorbed by beamsplitter, transmission is 45%.

7) Position 7: Optical power filtered by narrow-band filter is given by

$$P7=P6*(\Delta\lambda_{filter}/\Delta\lambda_{LED}) =0.36*(10nm/90nm) =0.04\mu w$$

Attenuation Cause: Output power from one branch of the beamsplitter is filtered by the narrow-band filter

8) Position 8: Current converted from optical power by the photodiode is given by

$$P8=P5*R =0.36uw*0.5uA/uw =0.18uA$$

where R is Responsivity of Photodiode.

Attenuation Cause: Conversion from optical power to electric current causes some attenuation because the Responsivity of Photodiode is less than 1

9) Position 9: Current converted from optical power by the photodiode is given by

$$P9=P7* R =0.04uw*0.5uA/uw =0.02uA$$

where R is Responsivity of Photodiode.

Attenuation Cause: Conversion from optical power to electric current causes some attenuation because the Responsivity of Photodiode is less than 1

Here one key point about the calculation above should be paid attention to. According to the principle of the Fabry-Parot Interferometer, the reflected interference optical power from the sensor head at position 2' will be greater than that from a just well-cleaved fiber endface in the calculation above. The maximal value of the optical power at position 2' will be four times the value we are currently using above.

### 3.5 Design and Implementation of Electric Circuit

The electric circuit part consists of the following components:

(1) Operational Amplifier (Analog Devices Corp., AD795)

(2) Power Supply @ ±12, 800mA (AAK Corp., MT12.8-.8)

(3) Laser Diode driver @ 200 mA (Wavelength Electronics, Inc., PLD-200)

### 3.5.1 Design and Implementation of Transimpedance Front-End

In design and implementation of the multimode fiber-based SCIIB sensor system, one important job is focused on the design and implementation of the optical receiver for optoelectronic conversion and signal amplification. Here lies in the one key noise source in the SCIIB sensor system. The most important circuit in the optical receiver is the current to voltage amplifier used to amplify the current. The combination of the photodetector and the preamplifier is called the receiver front-end [24]. The most popular front-end technology used in optical receivers is transimpedance front-end due to its optimum trade-off between noise, dynamic range and bandwidth. Other types of pre-amplifiers include high-impedance and low-impedance (e.g. 50 W) designs.

The basic electronic circuit of the transimpedance frond-end used in our sensor system is shown in Figure 3-4. The schematic includes the photodetecto r(PD) and pre-amplifier elements.

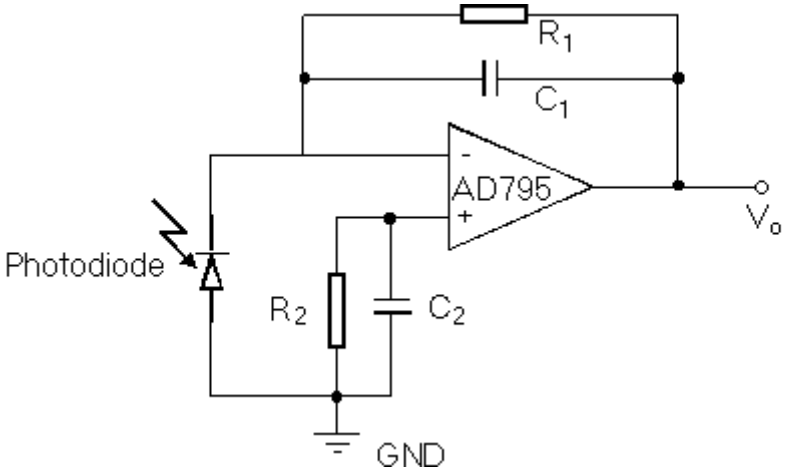


Figure 3-4. Schematic of transimpedance frond-end

The key performance requirements of the front-end are high sensitivity, wide dynamic range and adequate bandwidth for the intended application. The purpose of the PD is to

convert the incident optical signal to an electrical current. The photodiode should have the following performance characteristics: high responsivity (quantum efficiency), low dark current, low capacitance and wide bandwidth. The purpose of the pre-amplifier is to convert the photocurrent from the PD into a usable voltage that can be further processed.

The front-end schematic shown in Figure 3-4 converts the input optical power, $P_{in}$, into an electrical voltage given by

$$V_o = P_{in} R R_1 \qquad (3\text{-}1)$$

where R is the PD responsivity and $R_1$ is the feedback resistor in the amplifier. In our case, $R_1$ is 10MΩ and 1 MΩ for the Narrow Band and the Broad Band, respectively. According to the former power budget analysis, Vo ≈ 1 volt for both the Narrow Band and the Broad Band, which is within the ±5 volts sampling range of the data acquisition system.

The bandwidth, $f_c$, of the optical receiver can be approximated [25] by:

$$f_c = \frac{1}{2\pi R_1 (C_d + C_{in} + C_1)} \qquad (3\text{-}2)$$

where $R_1$ is the feedback resistance, $C_{in}$ is the input capacitance of the amplifier plus any parasitic capacitance, and $C_d$ is the PD capacitance, $C_1$ is the feedback capacitance of the amplifier. In our case, $C_{in}$ is 2pF, $C_d$ is 2300pF and $C_1$ is 1000pF, thus $f_c \approx 4.8$ Hz and 48Hz for the Narrow Band and the Broad Band, respectively.

According to the analysis above, the low photocurrent requires an amplifier with very high input impedance and a low bias current. The Analog Devices Inc.'s AD795 FET operational amplifier possesses these characteristics. The bias current of the AD795 is on the order of femtoamps and the input impedance is approximately 1011 ohms, which is sufficiently high for amplifying the photocurrent. A low noise metal film resistor made by Victoreen was used for the feedback resistor of the AD795 operational amplifier. The

stray capacitance between input Pin 2 and output Pin 6 of the AD795 is less than one picofarad.

The scale of the Printed Circuit Board(PCB) should be reduced as compact as possible to reduce parasitic effect and coupled noise. Two small PCBs we build for the Narrow Band and the Broad Band are soldered with the pins of photodiodes directly without coaxial cables. The photodiodes are packaged into a small optical box built for containing the beamsplitter, the optical filter and the photodiodes.

Proper layout and construction of the transimpedance amplifier are essential to maintaining high current sensitivity, low noise, and sufficient bandwidth. Leakage currents can destroy the high sensitivity of the AD795. To minimize the effects of leakage currents, the AD795 inverting input pin is guarded and both inputs are isolated from the printed circuit board with Teflon. The connection between the AD795 and the photodiode pin also deserves special attention. This connection should be as short as possible for several reasons. First, vibration of the connection wire can create piezoelectric effects and friction can create triboelectric charges. Second, a shorter connection also lowers susceptibility to stray fields and parasitic capacitance. The PCB is grounded with the SCIIB enclosure. This grounding method reduces the effective input capacitance and thus any noise generated by the "microphone effect." Third, we use a small shielding box covers all of the optical box and two small PCBs to avoid outside electromagnetic interference.

### 3.5.2 Analysis of Noise

Noise of the front-end includes noise from the photodiode and the amplifier. Major noises in the photodiode are the Shot Noise and Thermal Noise. As a photodiode amplifier, the current-to-voltage converter exhibits a complex noise behavior. Basic noise components

result from the circuit's feedback resistor and the amplifier input's noise current and noise voltage.

### 3.5.2.1 Noise in Photodiode

i) Shot Noise [24]

The shot noise can be associated with either the quantization of charge into multiples of q or, equivalently, with the quantization of light energy into photons (*q* is the charge on an electron $1.6\times10^{-19}$ C). The arrival of photons or, equivalently, the generation of charge carriers is characterized by Poisson statistics. The mean square noise current

$$I_s = \sqrt{2qI_{dc}\Delta f} \qquad (3\text{-}3)$$

where $I_{dc}$ is the average direct current, q is the electron charge, and $\Delta f$ is the bandwidth of the electronics accepting the noise (e.g., a preamplifier, a noise meter). The interpretation of the equation is that there is this much noise power in the frequency region extending from $f_0 - (\Delta f/2)$ to $f_0 + (\Delta f/2)$, where $f_0$ is the center frequency of the passband of the output device. Note also that, since $I_s$ is independent of the central frequency, the noise is white noise (i.e., the noise has a uniform frequency distribution).

The dc current $I_{dc}$ out of a PIN photodiode is made up of three components:

$$I_{dc} = I_L + I_{background} + I_{dark} \qquad (3\text{-}4)$$

where $I_L$ is the load current due to the incident light, $I_{background}$ is the current due to background illumination sources, and $I_{dark}$ is the dark current of the device. The dark current is the output of the device with no input illumination and is primarily due to thermal generation of charge carriers in the depletion region and surface leakage currents due to surface defects near the edges of the semiconductor.

Typically, the dark-current density is $10^{-6}$ – $10^{-7}$ A/cm2 in silicon devices, is $10^{-4}$ – $10^{-6}$ A/cm$^2$ in InGaAs, and is $10^{-3}$ A/cm$^2$ in Ge. The high dark current of the long-wavelength detectors causes their noise characteristics to be inferior to the short-wavelength silicon-based devices.

ii) Thermal Noise [24]

The second noise source of importance in photodiodes is thermal noise. Any resistive load or device with an associated resistance will produce a thermal-noise mean square current given by

$$I_t = \sqrt{\frac{4k_b T \Delta f}{R}} \qquad (3\text{-}5)$$

where $k_b$ is Boltzmann's constant, T is the noise temperature of the device, Δf is the electronic bandwidth into which the noise is delivered, and R is the value of the resistor or input resistance. This noise is independent of the optical signal.

### 3.5.2.2 Noise in Amplifier

i) Input Noise Current of Amplifier [25]

Noise current $i_{ni}$ represents the shot noise of the input bias current $I_{B-}$ and has a noise density of $i_{ni} = \sqrt{2qI_{B-}\Delta f}$ , where q is the charge on an electron, $1.6 \times 10^{-19}$ C. This noise current flows directly through the feedback resistor, producing a noise voltage of $e_{noi} = R_f \sqrt{2qI_{B-}\Delta f}$ . Like the noise voltage of $R_f$ itself, this new noise voltage transfers to the circuit output with unity gain. Choosing an operational amplifier with an $I_{B-}$ in the picoamp range generally makes this noise component negligible for practical levels of feedback resistance. The input noise current of AD795 is just 13 fA peak-to-peak from 0.1Hz to 10Hz.

ii) Input Noise Voltage of Amplifier [25]

In a more complex relationship, the amplifier's input noise voltage $e_{ni}$ receives an amplification characterized by a noise gain peaking. Within the open-loop gain response boundary of the operational amplifier, the output noise density $e_{noe}$ due to $e_{ni}$

$$e_{noe} = \frac{1 + R_f C_i s}{1 + R_f C_f s} e_{ni} \qquad (3\text{-}6)$$

where $C_i$ is the capacitor of the photodiode, and $C_f$ is the feedback capacitor. This will be a high frequency noise when the capacitors dominate the noise gain. For the AD795 amplifier, $e_{ni}$=3μv below 10Hz.

#### 3.5.2.3 Total Voltage Noise in Transimpedance Front-end

The total voltage noise ($e_{no}$) can be calculated by adding the contributions of all the above noises. Because these noises are independent random processes which can be approximately modeled by Gaussian statistics, the total variance of voltage fluctuation at the output of the transimpedance amplifier can be obtained by adding individual variances. Therefore, the combined output voltage noise of all the components is given by

$$e_{no} = \sqrt{(I_s R_f)^2 + (I_t R_f)^2 + e^2_{noi} + e^2_{noe}} \qquad (3\text{-}7)$$

### 3.6 Design and Implementation of Interface to Computer

The data acquisition system used for the sensor system is low-cost multifunction I/O board 5500MF and its companion — ADLIB WIN Interface Library Software for programming the software graphic user interface to the 5500MF.

### 3.6.1 Hardware of Data Acquisition System

The 5500MF Data Acquisition Board is provided by American Data Acquisition Corporation(ADAC). It is a data acquisition module for the IBM PC/XT/AT and PS/2 Model 30. The 5500MF is a half size module with 8 high level(±10 Volts) pseudo-

differential analog inputs multiplexed to a 12 bit A/D converter. Total hardware conversion time is approximately 30 microseconds; maximum throughputs of 25kHz can be achieved when operating under program control. The module also has 16 lines of TTL level digital I/O, the 5500MF contains an 8254 counter/timer chip which provides the board with three programmable timers, two of which can be used as input counters. This Counter/Timer feature allows the 5500MF to be used in pulse generation, timing, and counting applications.

### 3.6.2 Software of Data Acquisition System

ADLIB WIN is a set of sophisticated, high level, dynamically linked library (DLL) data acquisition subroutines for programmers involved in the developing of process and/or data acquisition applications. ADLIB WIN supports Microsoft C, Visual C++ and Visual Basic with a true 32 bit interface Windows 95/98 and a 16 bit interface for Windows 3.1. ADLIB supports DMA, Interrupt and Software Polled data transfer methods for acquiring data.

A computer program written in Visual Basic language is developed for the graphic user interface to 5500MF card and the Multimode fiber-based SCIIB Optical Fiber Temperature Sensor System. The illustrations of the Graphic User Interface(GUI) are shown in the following figures.

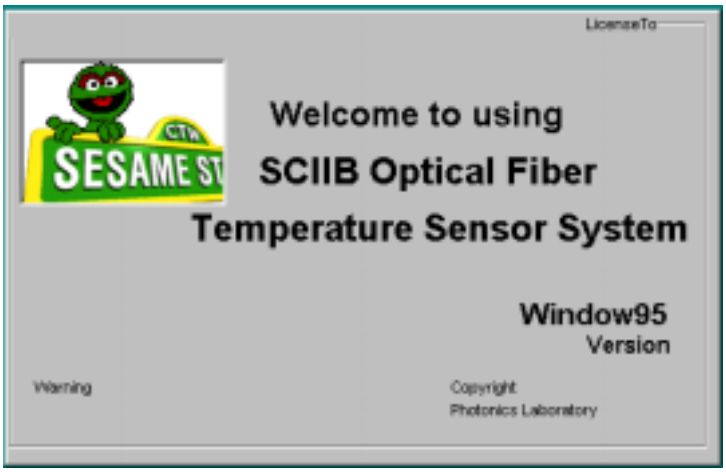


Figure 3-5. Illustration of GUI to the Multimode SCIIB Temperature Sensor System

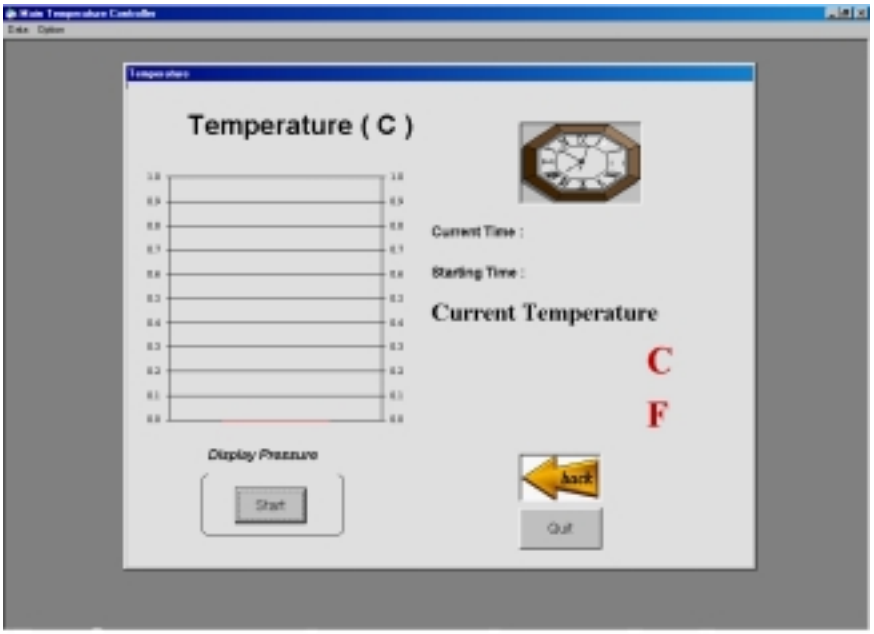


Figure 3-6. Illustration of GUI to the Multimode SCIIB Temperature Sensor System

### 3.7 Configuration of the Total Multimode SCIIB Temperature Sensor System

The SCIIB Temperature Sensor System consists of three parts – Sensor Head, SCIIB Instrument Box and 5500MF Data Acquisition Board(DAB) & computer. The sensor head converts the temperature signal to the change of the F-P cavity length. The SCIIB instrumentation box provides the information about the F-P cavity length change. The 5500MF ADC module samples the electrical signals output from the SCIIB instrumentation box and converts them to digital data. The computer is used to coordinate the operation of the system and perform necessary signal processing functions to allow the display and storage of the measured temperature data. In addition to the digital data files stored in the host computer, the system also provides an analog output which is proportional to the measured temperature.

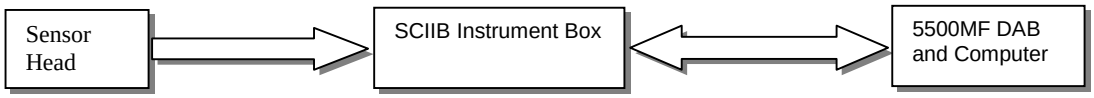


Figure 3-7. Schematic of Configuration of Multimode SCIIB Temperature Sensor System